

Radical Activation of Ammonia and Water at Bismuth(II)

Xiuxiu Yang¹, Edward J. Reijerse^{2‡}, Kalishankar Bhattacharyya^{1‡}, Markus Leutzsch¹, Markus Kochius¹, Nils Nöthling¹, Julia Busch¹, Alexander Schnegg², Alexander A. Auer¹, Josep Cornella^{1*}

ABSTRACT: The development of unconventional strategies for the activation of ammonia (NH₃) and water (H₂O) is of capital importance for the advancement of sustainable chemical strategies. Herein we provide the synthesis and characterization of a Radical Equilibrium Complex based on bismuth featuring an extremely weak Bi–O bond, that permits the *in situ* generation of reactive Bi(II) species. The ensuing organobismuth(II) engages with various amines and alcohols and exerts an unprecedented effect onto the X–H, leading to low BDFE_{X–H}. As a result, radical activation of various N–H and O–H bonds—including ammonia and water—occurs in seconds at room temperature, delivering well-defined Bi(III)-amido and -alkoxy complexes. Moreover, we demonstrate that the resulting Bi(III)–N complexes engage in a unique reactivity pattern with the triad of H⁺, H[–] and H[•] sources, thus providing alternative pathways for main group chemistry.

Introduction

Ammonia (NH₃) and water (H₂O) are ubiquitous small molecules that represent one of the pillars from which life on Earth sustains.¹ Due to their widespread presence, they have been identified as energy units or economic building blocks *en route* to high-value compounds.² However, their chemical manipulation is non-trivial, as a result of the high bond dissociation free energy (BDFE) of their N–H and O–H bonds (BDFE_{O–H} in H₂O = 113.0 kcal·mol^{–1}; BDFE_{N–H} in NH₃ = 100.3 kcal·mol^{–1}).³ Indeed, the majority of the approaches towards X–H cleavage focus on polar pathways; for example, both *d*- and *p*-block elements undergo oxidative addition⁴ or deprotonation through metal-ligand cooperation^{4c, 5} using the two-electrons of the respective *d*- and *p*-orbitals (Fig. 1A). More recently, the activation of the X–H bond through radical pathways has become feasible, albeit comparatively less examples are known. Although *s*-block elements can activate X–H bond through single-electron transfer (SET),⁶ milder strategies capitalizing on the concept of coordination-induced bond weakening have recently arisen (Fig. 1B).⁷ Examples of this reactivity are found in biology,⁸ catalysis,⁹ coordination chemistry^{7a} or ammonia synthesis.¹⁰ Yet, such reactivity is largely dominated by transition metals, and examples dealing with main group elements remain rare.^{11, 12} For example, a germanium corrole complex (group 14) has been reported to activate N–H and O–H bonds under UV light and in the presence of a large excess of organic substrate.^{11a, 13} Without irradiation, low yields were obtained at higher temperatures and extended reactions times. In the group 13, boron-containing compounds have been shown to lower the BDFE of E–H, including H₂O and NH₃.^{11b–e} Despite these examples, complexes based on group 15 elements that enable selective, fast, and mild radical activation of O–H and N–H bonds through coordination-induced bond weakening properties are still elusive.

As the heaviest stable element,¹⁴ the electronic structure of bismuth (Bi) is strongly influenced by relativistic effects, thus decreasing the energies of its 6*s* and 6*p* orbitals. Consequences of this unique electronic features are the well-known inert-pair effect¹⁵ or the strong Lewis acidity.¹⁶ In certain cases, homolysis

of RBi–X bonds becomes feasible due to the preferential stability of the RBi radical over the ionized heterolysis product RBi⁺.¹⁷ In principle, if the RBi[•] and X[•], generated from homolysis are stable, it is possible that this complex exists in both diamagnetic and paramagnetic form: a Radical Equilibrium Complex (REC) (Fig. 1C).¹⁸ Examples of Bi REC are scarce, and the few reported homolysis cases of the Bi–X bond are mainly irreversible, due to the high reactivity of the ensuing Bi radical species.¹⁹ Fundamental studies on a Bi–Mo catalyst for the SOHIO process conducted by Hanna suggested that Bi(II) intermediates—formed after thermal homolysis of the Bi(III) bearing bulky phenolates—could be responsible for the formation of allyl radicals from propene.^{19c} Similar reactivity with bulky phenolate anions was later observed by Evans in a unique C–H bismuthylation of phenols.^{19a} In 2018, Coles demonstrated that the Bi(III)–O bond in a R₂Bi–OTEMP compound is in equilibrium with the corresponding R₂Bi(II) and TEMPO[•].²⁰ Collectively, these precedents pointed to a facile thermal Bi–O bond scission of bulky oxy-type anions that can stabilize O centered radicals.^{19d, g} Yet, the origin and factors that influence this process still remain unclear and investigations on such unusual chemical properties would be desirable. Herein we report on the synthesis, reactivity and structural characterization of a Bi REC, whose Bi–O homolyzes reversibly at room temperature without the need for irradiation (Fig. 1D). We demonstrate that such complex permits fast, and mild activation of ammonia and water—among other alcohols and amines—resulting in well-defined Bi(III) amido and alkoxy compounds. We suggest that upon coordination to Bi(II), amines and alcohols undergo X–H bond weakening, thus permitting their facile radical activation. In addition, we propose that the novel pincer-based Bi(III)–NR₂ compounds show reactivity with a triad of H⁺, H[–] and H[•] sources. This rich and broad reactivity opens the door to the design of strategies for transferring and manipulating the NH₂ moiety upon ammonia activation, a highly coveted and important process toward considering NH₃ as viable building block.

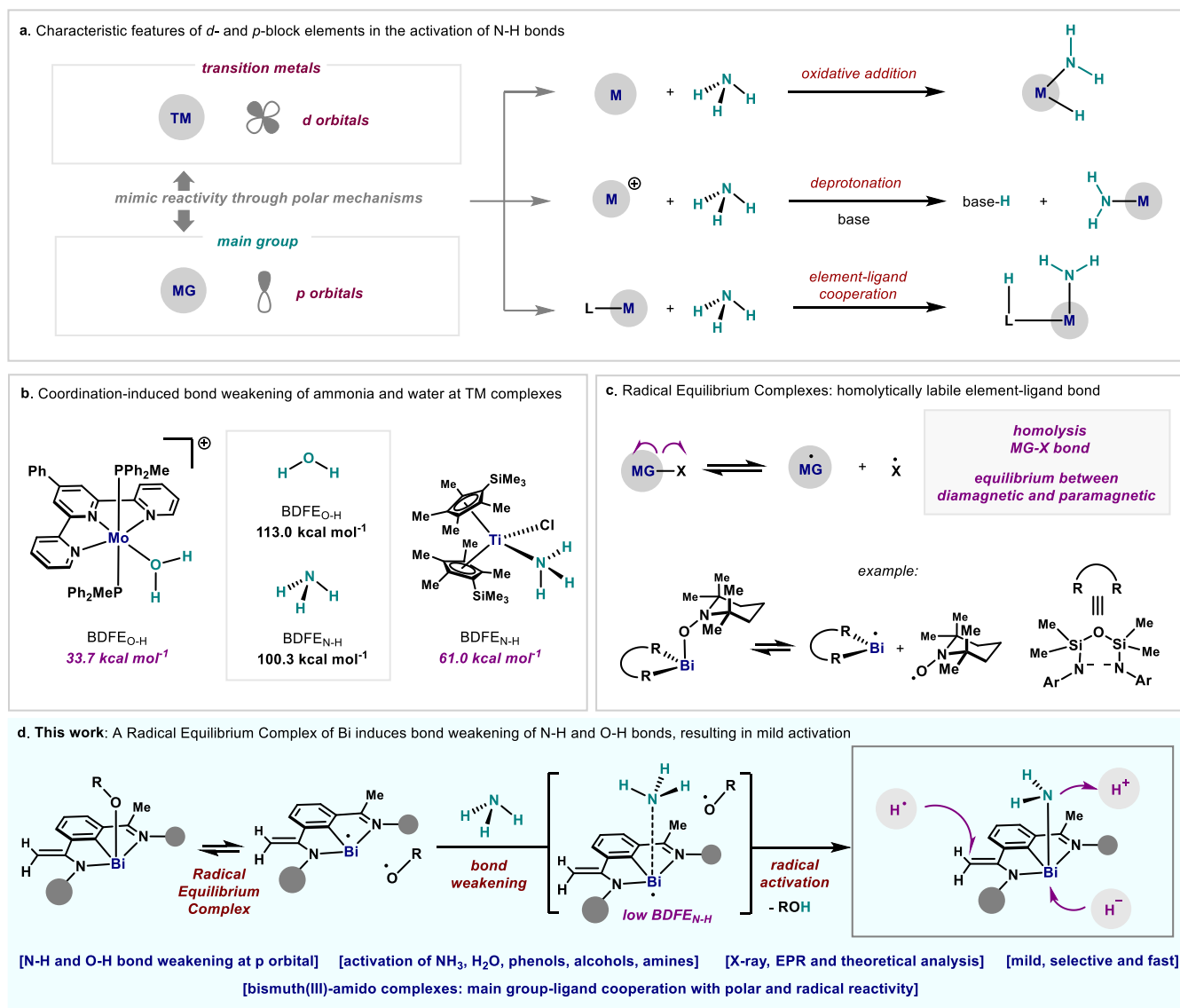


Figure 1. Overview of NH₃ and H₂O activation modes. **a.** State-of-the-art modes for NH₃ and H₂O activation by transition metals and main group elements. TM, transition metal. MG, main group element. **b.** Bond weakening of N–H and O–H by coordination to transition metal complexes. **c.** Left: reversible homolysis of MG–X single bond in Radical Equilibrium Complex (REC); right: example of a Bi REC (right).²⁰ **d.** This work: activation of NH₃ by a Bi–O REC complex, and reactivity of the Bi-amido products. TM: transition metal; MG: main group element.

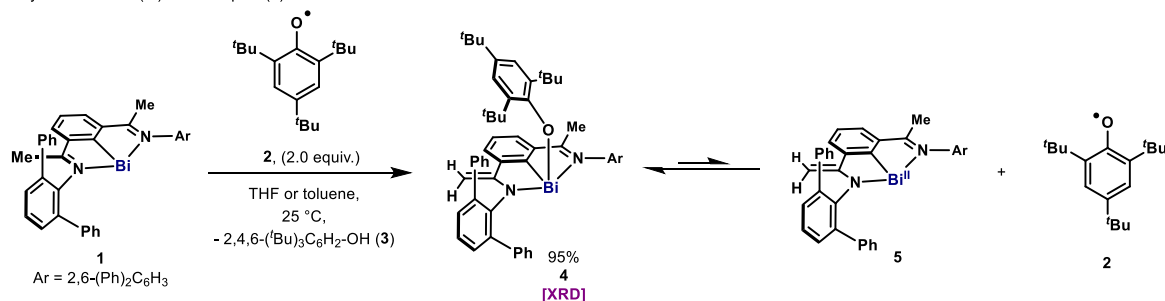
Results and discussion

Reaction of *N,C,N* organobismuth(I) **1** with 2.0 equiv. of alkoxide radical **2** in THF, led to the isolation of **4** in 95% yield as an orange solid, with concomitant formation of **3** (Fig. 2A). Single crystal XRD reveals **4** as monomeric structure and a fourfold coordinated Bi center (Fig. 2B, and SI). The bond distances of C7–C8 (1.355(6) Å) and C7–N1 (1.379(5) Å) clearly indicate a double C=C bond and a single C–N bond, respectively. The angles between Bi with the distinct three anionic ligands (C1, N1, O) vary from 75.48(13)° to 95.07(12)°, with a sum of angles up to 256.2°, pointing to a major contribution of the 6*p* Bi orbitals in the Bi–X bonds (X = C1, N1, O).²¹ Importantly, the Bi–O distance is considerably large (2.178(3) Å) and the angle of C47–O–Bi (136.2(3)°) is larger than the closely related BiCl(O–2,4,6–tBu₃C₆H₂).²² This implies a poor overlap

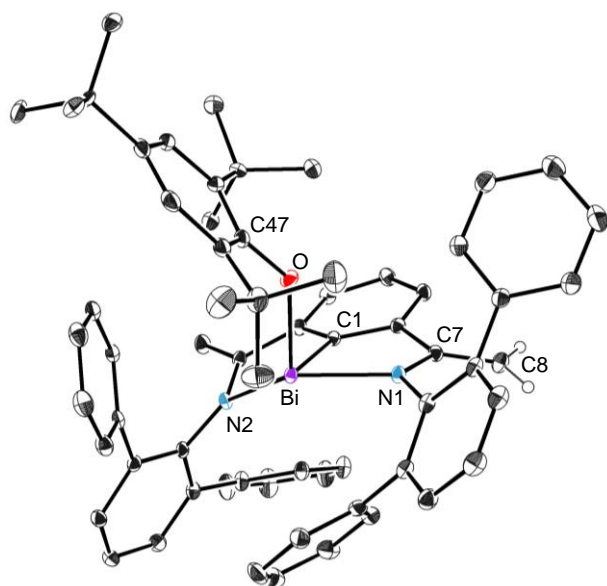
between the lone pair in the *sp*² hybridized orbital of the O atom and the diffuse *p* orbital of the Bi center, indicating a weak Bi–O bond. EPR analysis of **4** at room temperature resulted in the clear detection of the signal for the known radical **2** (Fig 2C, top),²³ which could be characterized with high resolution. Due to the relatively high temperature (>100 K) for the Bi–O bond homolytic cleavage, only **2** was detected, as the EPR signal for Bi(II) (**5**) is assumed to be too broad to be detectable, because of a fast relaxation caused by large spin-orbit coupling.^{19f} When **4** (13.08 mM) was subjected to successive cycles of temperature changes within the range of 243–293 K, the concentration of **2** remained constant at a given temperature, supporting the reversibility of the homolytic cleavage (see SI). The thermodynamic parameters of the equilibrium in PhMe ($\Delta H = +28.0 \pm 0.3 \text{ kcal}\cdot\text{mol}^{-1}$ and $\Delta S = +58.7 \pm 1.2 \text{ cal}\cdot\text{mol}^{-1}\cdot\text{K}^{-1}$) are consistent

with a dissociative mechanism (Fig. 2D, bottom).^{19f} Importantly, the large contribution of the entropy compensates for the unfavorable enthalpy and results in $\Delta G = +10.5 \pm 0.67$ kcal·mol⁻¹ at 298 K between the diamagnetic and the paramagnetic species. Computed singlet and triplet bond dissociation potential energy profiles of **4** at the PBE0/Def2-TZVP (ZORA)²⁴ level of theory are shown in Fig. 2D. Upon elongation of the Bi–O bond, the triplet state crosses the singlet state at around ~ 3.1 Å, indicating that splitting into two radical species is energetically favorable by 37.2 kcal·mol⁻¹. Spin density analysis indicates a considerable spin polarization on the Bi center when the Bi–O bond is elongated to 2.3 Å (see SI). Orbital analysis of the singlet state for **4** shows that the HOMO is predominantly located on the alkoxide ligand and the LUMO on the *N,C,N* ligand and neighboring Bi. The Bi–O cleavage is essentially completed at *ca* 4.5 Å. Importantly, values of $\Delta H = +25.0$ kcal·mol⁻¹ and $\Delta S = +62.1$ cal·mol⁻¹·K⁻¹ for the Bi–O scission are in good agreement with the experimental thermodynamic data obtained by EPR. The considerable entropic contribution is attributed to high translational and rotational entropy components resulting in a rather small computed $\Delta G = +6.5$ kcal·mol⁻¹ ($\Delta G_{exp} = +10.5 \pm 0.67$ kcal·mol⁻¹). In comparison, the heterolytic bond cleavage of the Bi–O bond, is highly endergonic with $\Delta G = +43.7$ kcal·mol⁻¹, supporting the energetic preference for the formation of radical **2** and **5**. It is important to highlight that the weak Bi–O bond is a consequence of the relativistic effect of Bi, which combined with the stability of the Bi(II) by the pincer framework, the stability of radical **2** and the large entropic gain, results in a mild homolytic cleavage.

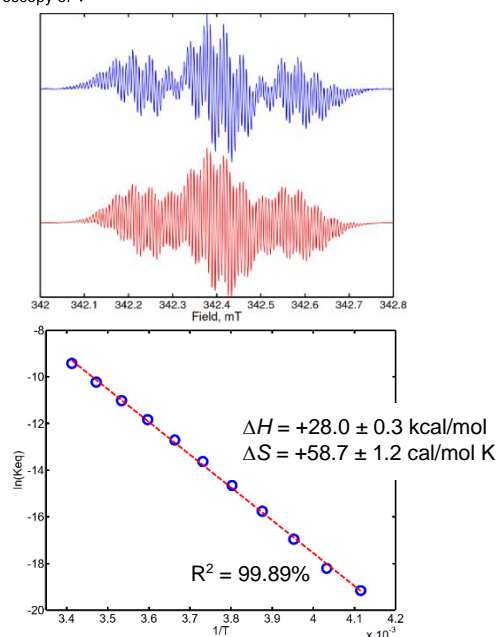
a. Synthesis of a Bi(III)-OAr complex (4)



b. X-ray of complex 4



c. EPR spectroscopy of 4



d. Computational analysis of 4

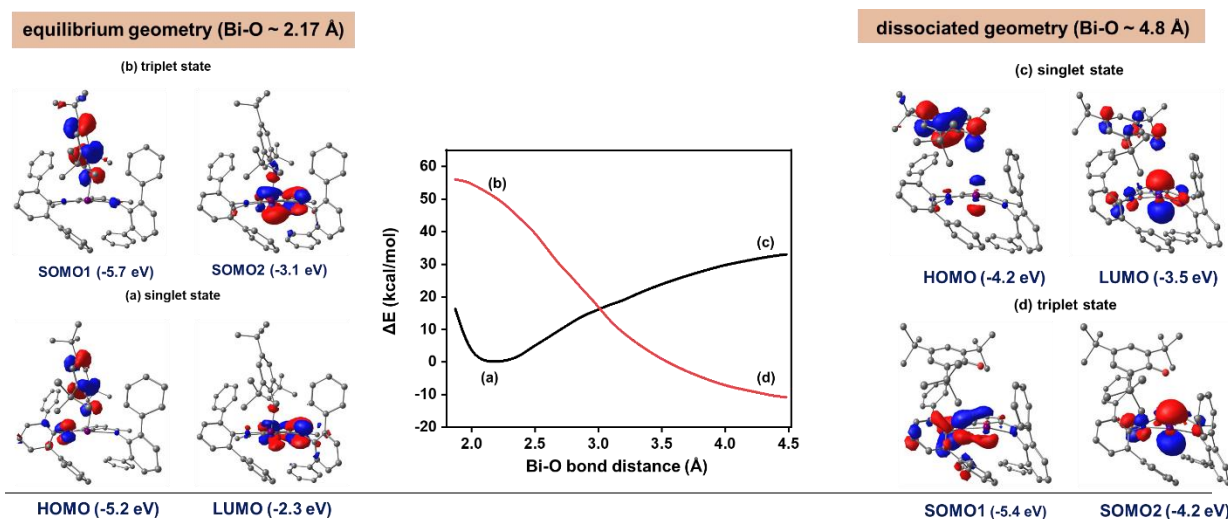


Figure 2. Synthesis and characterization of a bismuth radical equilibrium complex. a. Synthesis of complex 4. b. Solid-state structure of 4, illustrated using 30% probability ellipsoids except hydrogen atoms. Solvents, hydrogen atoms, and disordered parts have been omitted for clarity, except those on C8. c. top: EPR spectra of complex 4 (after dissociation) at 25 °C (blue line) spectral simulation (red line) parameters: $g = 2.00854$, $2 \times 1H-A = 4.76$ MHz, $9 \times 1H-A = 1.04$ MHz, $18 \times 1H-A = 0.2$ MHz; bottom: van't Hoff plot of 4 in PhMe between -30 °C and 20 °C. d. Computational analysis of the Bi-O bond cleavage: potential energy profiles of the Bi-O bond dissociation of 4 at (ZORA) PBE0-D3/Def2-TZVP (SMD:Toluene) level of theory. Black and red color denote singlet (heterolytic bond cleavage) and triplet (homolytic bond cleavage) potential energy surface. Frontier molecular orbitals both in singlet (a,c) and triplet states (b,d) are plotted at equilibrium (left panel) and dissociated (right panel) geometries.

The BDFE of X–H on a ligand is influenced by the oxidation potential at the metal center and a pK_a value of X–H.³ Therefore, coordination to Bi(II) will increase the population at the anti-bonding orbitals, making RBi(II)–X–H a strong reductant.¹³ Hence, the Bi(II)/Bi(III) redox couple presents itself as a good candidate for coordination-induced bond weakening. When **4** was mixed with 1.0 equiv. of phenol (**6**, $BDFE_{O-H} = 79.8 \text{ kcal}\cdot\text{mol}^{-1}$),³ rapid formation of **7** was obtained in 92% isolated yield (Figure 3). Interestingly, the reaction with 1.0 equiv. of H₂O ($BDFE_{O-H} = 113.0 \text{ kcal}\cdot\text{mol}^{-1}$) led to rapid conversion to the corresponding hydroxy bismuth **9** (86%), which has recently been characterized in the context of N₂O activation.²⁵ Cyclohexanol afforded the corresponding bismuth alkoxide **11** in 98% yield. Similarly, when primary α -monoalkyl (**12**, $BDFE_{N-H} = 95.0 \text{ kcal}\cdot\text{mol}^{-1}$) and α -dialkyl amines (**14**, $BDFE_{N-H} = 90.7 \text{ kcal}\cdot\text{mol}^{-1}$) were mixed with **4**, the corresponding bismuth amides were obtained in 78% (**13**) and 95% (**15**) yields, respec-

tively. Similar yields were observed in apolar non-protic solvents, as shown for the 95% yield of **15** in PhMe. Finally, when **4** was mixed with 1.0 equiv. of dry ammonia, **17** was isolated in 76% yield. It is important to mention that Bi(III) complexes bound to a free NH₂ group are rare,²⁶ and therefore, **17** represents a unique example of such pnictogen-pnictogen bond. **7**, **9**, **11**, **13**, **15** and **17** are diamagnetic and no signal was detected by EPR in toluene at various temperatures. In all cases, solid-state structures reveal the bismuth center to be fourfold coordinated, and residing in a distorted plane formed by the imine, amido and phenyl ring (see SI). The –OH, –OPh, –NHCy, and –NH₂ groups in **7**, **9**, **15** and **17** are perpendicular to this plane, and they localize on either side. The bond distances of C7–C8 and C7–N1 clearly indicate that the double C=C bonds and single C–N bonds are preserved.

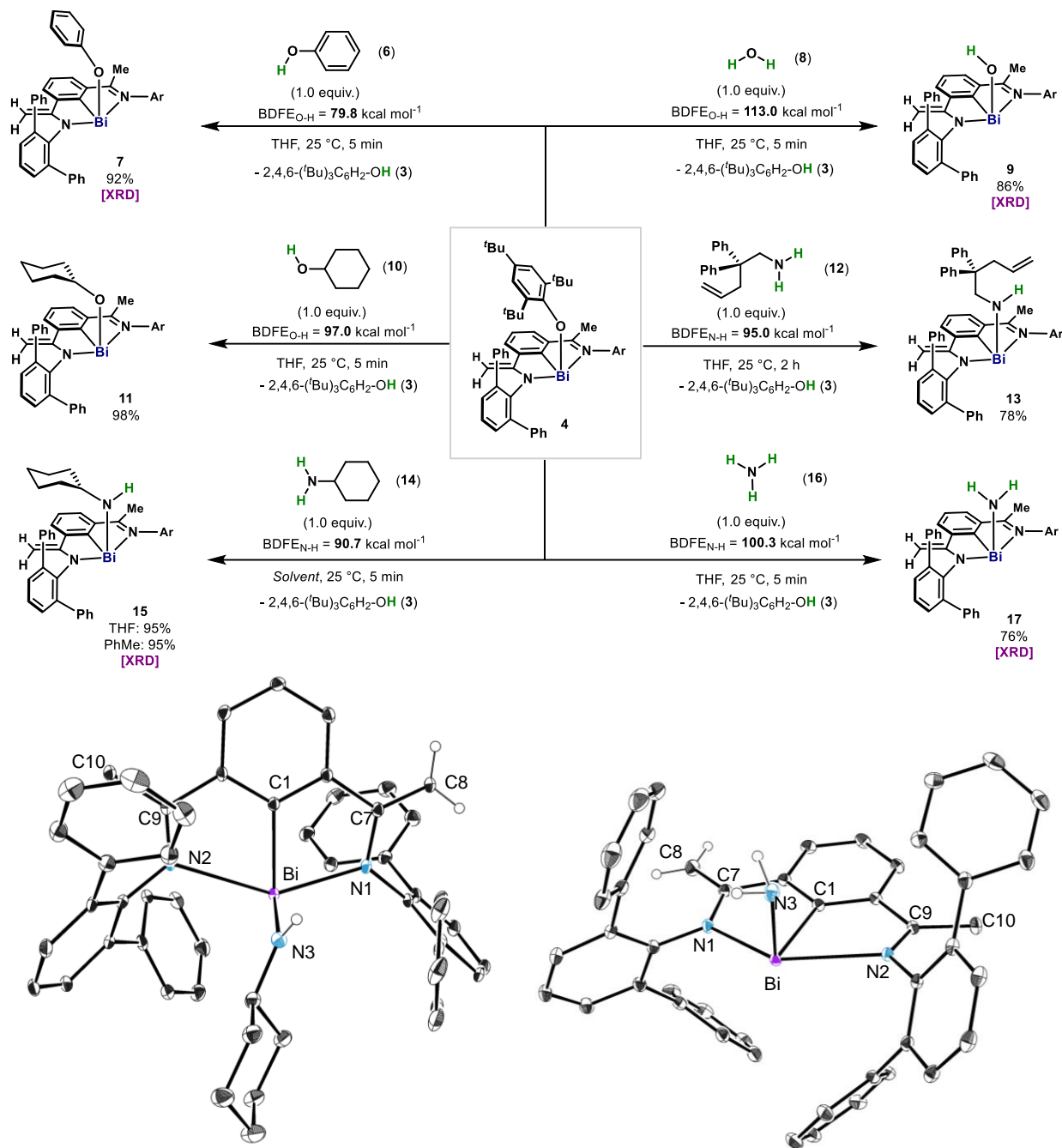
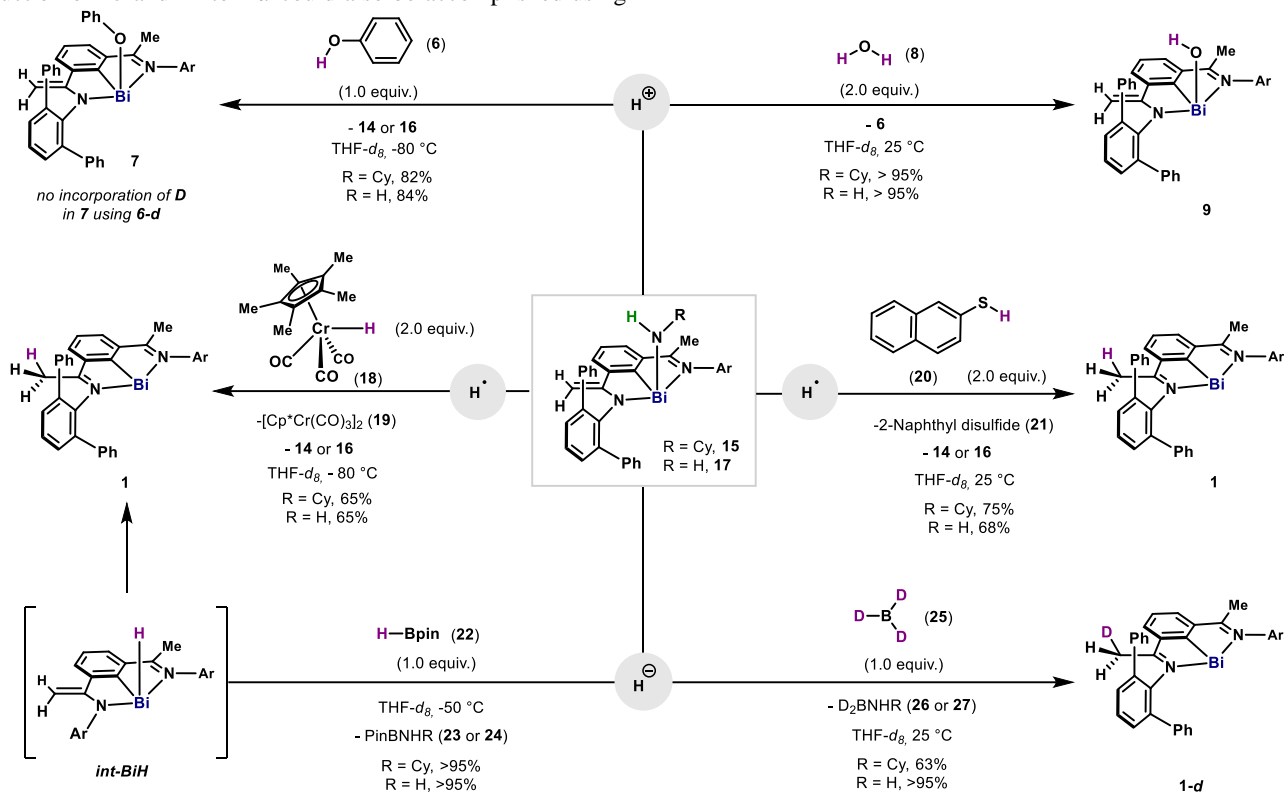


Figure 3. Activation of O–H and N–H bonds: synthesis of **7**, **9**, **11**, **13**, **15**, **17** (top), and solid-state structure of **15** (bottom, left) and **17** (bottom, right), illustrated using 30% probability ellipsoids except hydrogen atoms. Solvents, hydrogen atoms, except those on C8 and N3 in **15** and **17**, and disordered parts have been omitted for clarity. All yields are of isolated pure material.

Generally, main group elements beyond group 14 have a reduced tendency to form stable complexes with NH₃;^{5b} and therefore represent excellent candidates for NH₃ activation and direct conversion to added-value chemicals beyond the stable MG–NH₂ compounds.²⁷ In order to explore their reactivity, **15** and **17** were mixed with various X–H sources (Scheme 1). Initially, the basicity of the Bi–NH₂ and Bi–NHCy bond was confirmed by the immediate reaction at –80 °C with **6**, leading to **7** and **14/16**. Such basicity is also demonstrated by the reaction with H₂O, leading quantitatively to **9**. When **6** was replaced by **6-d**, no deuteration of the ligand was observed, pointing to reactivity occurring solely at the Bi center. Additionally, when **15** and **17** were mixed with a chromium hydride with a weak Cr–

H bond (**18**) (BDFE_{Cr–H} = 53.0 kcal·mol^{–1}),²⁸ reduction to **1** rapidly occurred at –80 °C, with no intermediates detected. Concomitantly, Cr–Cr dimer **19** and **14/16** resulted, which point to a radical reaction of **15** and **17** with a weak H[•] source.^{19d, e} **1** was also produced selectively when **15** and **17** were mixed with 2 equiv. of 2-naphthalenethiol (**20**) (BDFE_{S–H} = 75.9 kcal·mol^{–1}, see SI), which formed 2-naphthyl disulfide (**21**) and **14/16**.²⁹ Interestingly, when **15** and **17** were mixed with an alternative hydride source with a much larger BDFE_{B–H} = 108.6 kcal·mol^{–1},³⁰ reduction to **1** occurred with the formation of **21/22**. However, in this case, a Bi(III)–H (*int-BiH*) could be detected at –50 °C, featuring the characteristic signal in the ¹H NMR at +26.0

ppm.³¹ *Int-BiH* slowly converted into **1** at $-50\text{ }^{\circ}\text{C}$, with the migration of the H atom to the methylene backbone. Incorporation of one deuterium in the methyl groups on the backbone using DBpin further confirmed such migration (see SI). Moreover, reduction of **15** and **17** to **1-d** could also be accomplished using



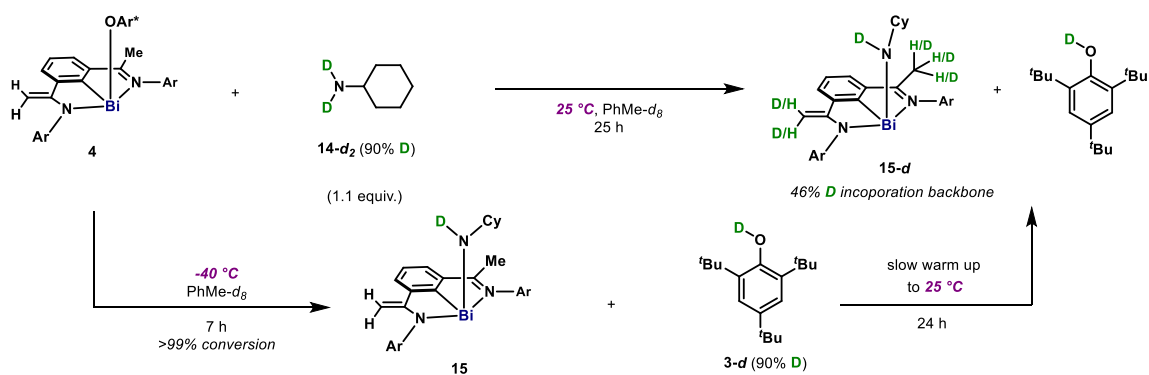
Scheme 1. Reactivity of bismuth(III) amido complexes **15** and **17** with H^+ , H^- and H^\bullet sources. Ar = 2,6-diphenylphenyl.

As shown in **15** and **17**, element-ligand cooperation through the methylene unit is feasible during radical and hydride processes involving H. To evaluate whether similar reactivity is involved in the activation of N–H bonds, we carried out the activation of cyclohexylamine deuterated (**14-d₂**, 90% D) using **4**. As shown in Fig. 4A, both methyl and methylene moieties resulted in an enrichment of deuterium (46% D) after 25 h at $25\text{ }^{\circ}\text{C}$. However, when the reaction was carried out at $-40\text{ }^{\circ}\text{C}$ and monitored by NMR, no obvious incorporation of D in the backbone was detected after complete conversion to **15**. Only upon warming the reaction mixture to $25\text{ }^{\circ}\text{C}$, a clear exchange of H for D in the CH_3 and CH_2 could be detected. These experiments confirm: 1) the absence of H/D exchange on the ligand by **14-d₂** during X–H activation; 2) and that ligand non-innocent reactivity with **3-d** is triggered at higher temperatures from amido complex **15**. Fig. 4B contains the computed free energy profile for the N–H bond activation step (green-dotted line). Based on the combined experimental evidence and the computational analysis, it is proposed that upon reversible homolysis of the Bi–O bond in **4**, NH_3 coordinates to the Bi(II) radical through the semi-occupied $6p_z$ orbital to generate **II**. HAT from **II** to OAr radical (**2**) proceeds with a very low energy barrier ($\text{TS}^{\text{II-III}}$, $\Delta G = +1.3\text{ kcal}\cdot\text{mol}^{-1}$), resulting in **III** ($\Delta G = -4.3\text{ kcal}\cdot\text{mol}^{-1}$). The low energy barrier associated with $\text{TS}^{\text{II-III}}$ is the result of the remarkably low $\text{BDFE}_{\text{N-H}} = 47.0\text{ kcal}\cdot\text{mol}^{-1}$ calculated for

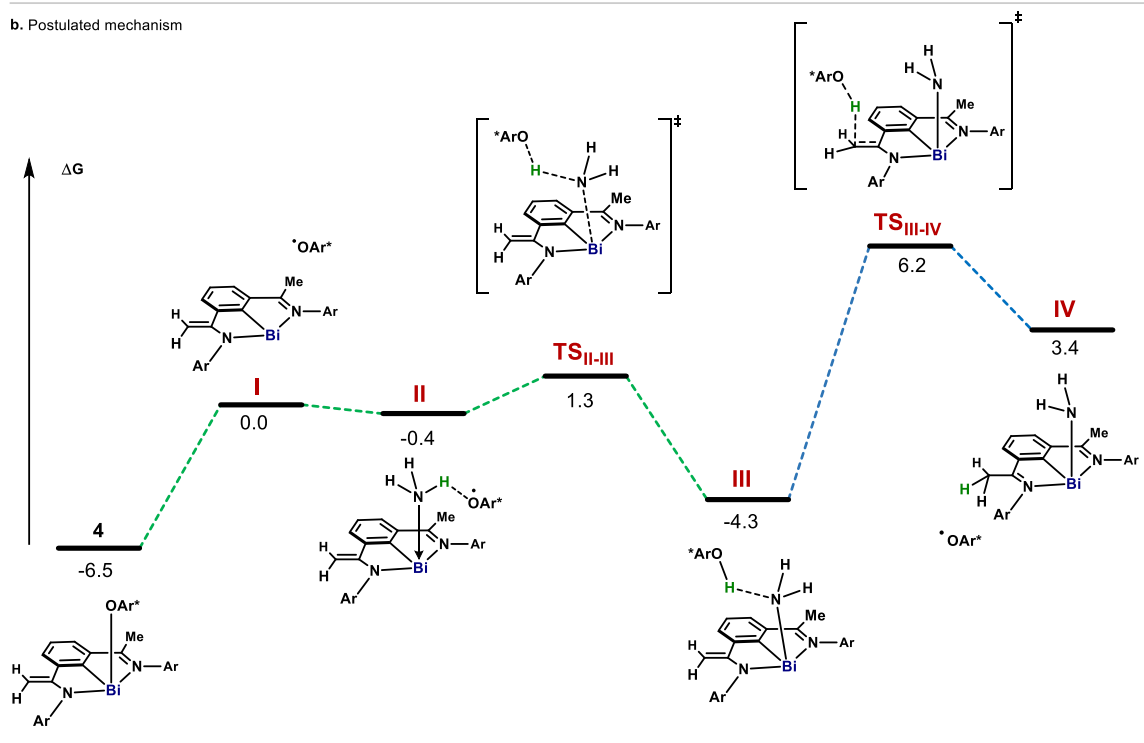
BD₃. Collectively, these bismuth-amido complexes feature chemically non-innocent reactivity (element-ligand cooperation),³² as well as reactivity towards radical species.

the N–H bond once coordinated to the Bi(II) center. Such coordination-induced bond weakening effect of the Bi(II) was also observed for H_2O , CyNH_2 and CyOH , with $\text{BDFE}_{\text{X-H}} = 52.1$, 59.1 , and $52.3\text{ kcal}\cdot\text{mol}^{-1}$, respectively (Fig. 4C, left). Without hydrogen bonding, **17** is significantly lower in energy ($-14.1\text{ kcal}\cdot\text{mol}^{-1}$) (see SI), permitting its isolation. The hydrogen exchange observed experimentally at the vinylic C–H bonds after the N–H activation was also computationally evaluated (Fig. 4B, blue-dotted line). The computed barrier for the radical hydrogen exchange between **III** and **IV** raises to $\Delta G^\ddagger = +10.5\text{ kcal}\cdot\text{mol}^{-1}$, due to the energetic mismatch between **IV** ($\text{BDFE}_{\text{C-H}} = +51.1\text{ kcal}\cdot\text{mol}^{-1}$) and **2** ($\text{BDFE}_{\text{O-H}} = +76.8\text{ kcal}\cdot\text{mol}^{-1}$)³ (Fig. 4C, middle). Upon single electron transfer (SET) between **1** and **2**, the Me C–H bond in the backbone in **V** also undergoes bond-weakening (Fig. 4C, right, $\text{BDFE}_{\text{C-H}} = +60.4\text{ kcal}\cdot\text{mol}^{-1}$),³³ resulting in feasible H-abstraction by **2 en route** to starting complex **4** (Fig. 2A). The small energy difference between **4** and **III** indicates that NH_3 activation might be reversible,^{5b} which was confirmed by the incorporation of deuterium in the CH_2 groups of **4** in the presence of ND_3 (see SI). Finally, alternative pathways such as direct HAT from **2** to NH_3 without the involvement of Bi, or reaction between **4** and NH_3 through heterolytic cleavage or polar pathways were discarded due to the highly endergonic profiles obtained ($>40\text{ kcal}\cdot\text{mol}^{-1}$, see SI).

a. Isotope labelling experiments: bismuth-ligand cooperation vs direct activation



b. Postulated mechanism



c. Bond Dissociation Free Energies

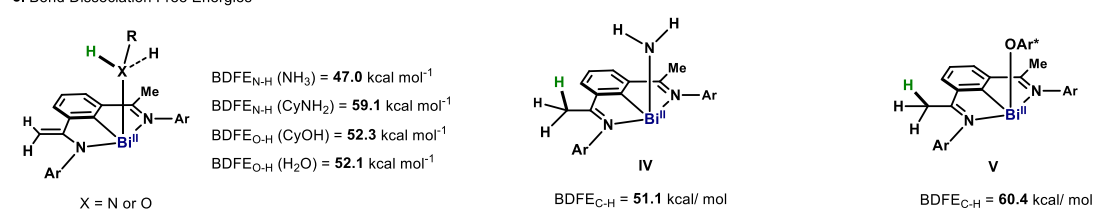


Figure 4. Mechanistic investigations. a. Deuterium labeling experiments at various temperatures. b. Theoretical analysis of the mechanism of the radical activation of N–H bond in ammonia. Computed free energy (ΔG , in kcal·mol⁻¹) profile for the N–H bond cleavage of NH_3 by $5'/\text{OAr}$ pair. Relative free energies (in kcal·mol⁻¹) are computed based on (ZORA) PBE0-D3/Def2-TZVP (SMD:Toluene) single point energies, and gas-phase free energies corrections at 298.15 K obtained at the (ZORA) BP86-D3/Def2-TZVP level of theory. c. Calculated BDFE of N–H and O–H bonds after coordination with Bi(II). $\text{OAr}^* = 2,4,6\text{-}(\text{tBu})_3\text{C}_6\text{H}_2\text{O}$

Conclusions

In this article, we disclose the design, synthesis and reactivity of a bismuth REC (**4**), featuring a weak Bi–O bond. The facile homolysis at room temperature leads to a highly reactive Bi(II) (**5**) with unusual chemical properties. Compound **4** is able to perform a rapid, selective and mild activation of ammonia and water—among other amines and alcohols—resulting in exclusive alkoxy- and amido-bismuth(III) complexes. Reactivity studies of the novel Bi(III)–NHR resulted in engagement with the triad of proton, hydride or radical hydrogen sources, a rather unique feature for main group elements. A combined experimental and computational analysis of the system suggests that upon homolysis, coordination of the lone pair in X–H to **5** occurs, resulting in a dramatic reduction of the BDFE_{X-H} and allowing its cleavage by the phenolate radical. Although Bi(III)–NHR have shown reactivity involving the ligand framework, deuteration experiments and kinetic analysis indicate that no element-ligand cooperation occurs during the activation, in agreement with the mechanistic hypothesis from a computational analysis. Properties such as coordination-induced bond weakening at bismuth combined with the rich reactivity pattern offered by the Bi(III)-amido complexes (at metal and ligand), could open the door to new possibilities for the conversion of cheap and abundant alcohols and amines into high-value compounds.

ASSOCIATED CONTENT

Supporting Information. This material is available free of charge via the Internet at <http://pubs.acs.org>.

The Supplementary Information contains all Experimental Procedures and analytical data (¹H, ¹³C, ¹⁵N NMR, HRMS, and crystallographic data) for all new compounds. Crystallographic data for compounds **4** (CCDC- 2128290), **7** (CCDC- 2128291), **15** (CCDC- 2128288), **17** (CCDC- 2128289) can be downloaded free of charge from the Cambridge Crystallographic Data Center www.ccdc.cam.ac.uk.

AUTHOR INFORMATION

Corresponding Author

Josep Cornella* Max-Planck-Institut für Kohlenforschung, Kaiser-Wilhelm-Platz 1, 45470, Mülheim an der Ruhr, Germany.
Email: cornella@kofo.mpg.de

Author

Xiuxiu Yang, Max-Planck-Institut für Kohlenforschung, Kaiser-Wilhelm-Platz 1, 45470, Mülheim an der Ruhr, Germany;

Edward J. Reijerse‡, Max-Planck-Institut für Chemische Energiekonversion, Stiftstrasse 34-36, 45470, Mülheim an der Ruhr, Germany;

Kalishankar Bhattacharyya‡, Max-Planck-Institut für Kohlenforschung, Kaiser-Wilhelm-Platz 1, 45470, Mülheim an der Ruhr, Germany;

Markus Leutzsch, Max-Planck-Institut für Kohlenforschung, Kaiser-Wilhelm-Platz 1, 45470, Mülheim an der Ruhr, Germany;

Markus Kochius, Max-Planck-Institut für Kohlenforschung, Kaiser-Wilhelm-Platz 1, 45470, Mülheim an der Ruhr, Germany;

Nils Nöthling, Max-Planck-Institut für Kohlenforschung, Kaiser-Wilhelm-Platz 1, 45470, Mülheim an der Ruhr, Germany;

Julia Busch, Max-Planck-Institut für Kohlenforschung, Kaiser-Wilhelm-Platz 1, 45470, Mülheim an der Ruhr, Germany;

Alexander Schnegg, Max-Planck-Institut für Chemische Energiekonversion, Stiftstrasse 34-36, 45470, Mülheim an der Ruhr, Germany;

Alexander A. Auer, Max-Planck-Institut für Kohlenforschung, Kaiser-Wilhelm-Platz 1, 45470, Mülheim an der Ruhr, Germany.

Author Contributions

‡These authors contributed equally to this work
X.Y. conducted all the experimental work. DFT calculations in this work were performed by K.B. under the supervision of A.A.A. and both provided the complete theoretical study. EPR experiments were conducted by E. J. R. and X.Y.; A. S. supervised and helped in the analysis and interpretation of the EPR data. M. L., M. K. and X. Y. carried out all NMR experiments and analysis. N. N. performed structure elucidation by XRD. J. B. aided in the synthesis of ligand scaffolds. J. C. conceived the idea, directed the project and wrote the manuscript.

Funding Sources

Financial support for this work was provided by Max-Planck-Gesellschaft, Max-Planck-Institut für Kohlenforschung, Max-Planck-Institute for Chemical Energy Conversion, Fonds der Chemischen Industrie (FCI-VCI). This project has received funding from European Union's Horizon 2020 research and innovation programme under Agreement No. 850496 (ERC Starting Grant, J.C.). K. B. is thankful to the Alexander von Humboldt Foundation for a postdoctoral Fellowship.

ACKNOWLEDGMENT

We thank Prof. Dr. A. Fürstner for insightful discussions and generous support. R. Goddard and J. Rust are acknowledged for structural discussions. We thank all the analytical departments at the MPI-Kohlenforschung for support in the characterization of compounds.

REFERENCES

- (1) (a) Smil, V. Detonator of the population explosion. *Nature* **1999**, *400*, 415-415. (b) Lewis, N. S.; Nocera, D. G. Powering the planet: chemical challenges in solar energy utilization. *PNAS* **2006**, *103*, 15729-15735.
- (2) (a) Service, R. F. Ammonia—a renewable fuel made from sun, air, and water—could power the globe without carbon. 2018. (b) Tullo, A. H. Is ammonia the fuel of the future? In *Chemical&Engineering News*, 2021; Vol. 99. (c) Kim, T. W.; Choi, K.-S. Nanoporous BiVO₄ photoanodes with dual-layer oxygen evolution catalysts for solar water splitting. *Science* **2014**, *343*, 990-994.
- (3) Agarwal, R. G.; Coste, S. C.; Groff, B. D.; Heuer, A. M.; Noh, H.; Parada, G. A.; Wise, C. F.; Nichols, E. M.; Warren, J. J.; Mayer, J. M. Free energies of proton-coupled electron transfer reagents and their applications. *Chem. Rev.* **2022**, *122*, 1-49.
- (4) (a) Zhao, J.; Goldman, A. S.; Hartwig, J. F. Oxidative addition of ammonia to form a stable monomeric amido hydride complex. *Science* **2005**, *307*, 1080-1082. (b) Frey, G. D.; Lavallo, V.; Donnadiu, B.; Schoeller, W. W.; Bertrand, G. Facile splitting of hydrogen and ammonia by nucleophilic activation at a single carbon center. *Science* **2007**, *316*, 439-441. (c) Klahn, M.; Beweries, T. Organometallic water splitting – from coordination chemistry to catalysis. *Rev Inorg Chem* **2014**, *34*, 177-198. (d) Robinson, T. P.; De Rosa, D. M.; Aldridge, S.; Goicoechea, J. M. E–H bond activation of ammonia and water by a geometrically constrained phosphorus(III) compound. *Angew. Chem. Int. Ed.* **2015**, *54*, 13758-13763. (e) Protchenko, A. V.; Bates, J. I.; Saleh, L. M. A.; Blake, M. P.; Schwarz, A. D.; Kolychev, E. L.; Thompson, A. L.; Jones, C.; Mountford, P.; Aldridge, S. Enabling and probing oxidative addition and reductive elimination at a group 14 metal center: cleavage and functionalization of E–H bonds by a bis(boryl)stannylene. *J. Am. Chem. Soc.* **2016**, *138*, 4555-4564. (f) Peng, Y.; Guo, J.-D.; Ellis, B. D.; Zhu, Z.; Fetting, J. C.; Nagase, S.; Power, P. P. Reaction of hydrogen or ammonia with unsaturated germanium or tin molecules under ambient conditions: oxidative addition versus arene elimination. *J. Am. Chem. Soc.* **2009**, *131*, 16272-16282. (g) Morgan, E.; MacLean, D. F.; McDonald, R.; Turculet, L. Rhodium and Iridium amido complexes supported by silyl pincer ligation: ammonia N–H bond activation by a [PSiP]Ir Complex. *J. Am. Chem. Soc.* **2009**, *131*, 14234-14236. (h) Jana, A.; Schulzke, C.; Roesky, H. W. Oxidative addition

- of ammonia at a silicon(II) center and an unprecedented hydrogenation reaction of compounds with low-valent group 14 elements using ammonia borane. *J. Am. Chem. Soc.* **2009**, *131*, 4600-4601.
- (5) (a) Gutsulyak, D. V.; Piers, W. E.; Borau-Garcia, J.; Parvez, M. Activation of water, ammonia, and other small molecules by PC_{carbene}P nickel pincer complexes. *J. Am. Chem. Soc.* **2013**, *135*, 11776-11779. (b) Abbeneth, J.; Townrow, O. P. E.; Goicoechea, J. M. Thermoneutral N-H bond activation of ammonia by a geometrically constrained phosphine. *Angew. Chem. Int. Ed.* **2021**, *60*, 23625-23629. (c) Meltzer, A.; Inoue, S.; Präsang, C.; Driess, M. Steering S-H and N-H bond activation by a stable N-Heterocyclic silylene: different addition of H₂S, NH₃, and organoamines on a silicon(II) ligand versus its Si(II)→Ni(CO)₃ complex. *J. Am. Chem. Soc.* **2010**, *132*, 3038-3046. (d) Kimura, T.; Koiso, N.; Ishiwata, K.; Kuwata, S.; Ikariya, T. H-H and N-H bond cleavage of dihydrogen and ammonia with a bifunctional parent imido (NH)-bridged diiridium complex. *J. Am. Chem. Soc.* **2011**, *133*, 8880-8883. (e) Khaskin, E.; Iron, M. A.; Shimon, L. J. W.; Zhang, J.; Milstein, D. N-H activation of amines and ammonia by Ru via metal-ligand cooperation. *J. Am. Chem. Soc.* **2010**, *132*, 8542-8543. (f) Cui, J.; Li, Y.; Ganguly, R.; Inthirarajah, A.; Hirao, H.; Kinjo, R. Metal-free σ-bond metathesis in ammonia activation by a diazadiphosphapentalene. *J. Am. Chem. Soc.* **2014**, *136*, 16764-16767. (g) Chang, Y.-H.; Nakajima, Y.; Tanaka, H.; Yoshizawa, K.; Ozawa, F. Facile N-H bond cleavage of ammonia by an Iridium complex bearing a noninnocent PNP-pincer type phosphalkene ligand. *J. Am. Chem. Soc.* **2013**, *135*, 11791-11794. (h) Brown, R. M.; Borau Garcia, J.; Valjus, J.; Roberts, C. J.; Tuononen, H. M.; Parvez, M.; Roesler, R. Ammonia activation by a Nickel NCN-pincer complex featuring a non-innocent N-Heterocyclic Carbene: ammine and amido complexes in equilibrium. *Angew. Chem. Int. Ed.* **2015**, *54*, 6274-6277.
- (6) Alan Sharpe, C. H. *Inorganic Chemistry 4th Edition*; Pearson, 2012.
- (7) (a) Bezdek, M. J.; Guo, S.; Chirik, P. J. Coordination-induced weakening of ammonia, water, and hydrazine X-H bonds in a molybdenum complex. *Science* **2016**, *354*, 730-733. (b) Pappas, I.; Chirik, P. J. Ammonia synthesis by hydrogenolysis of titanium-nitrogen bonds using proton coupled electron transfer. *J. Am. Chem. Soc.* **2015**, *137*, 3498-3501. (c) Margulieux, G. W.; Bezdek, M. J.; Turner, Z. R.; Chirik, P. J. Ammonia activation, H₂ evolution and nitride formation from a molybdenum complex with a chemically and redox noninnocent ligand. *J. Am. Chem. Soc.* **2017**, *139*, 6110-6113. (d) Cuerva, J. M.; Campaña, A. G.; Justicia, J.; Rosales, A.; Oller-López, J. L.; Robles, R.; Cárdenas, D. J.; Buñuel, E.; Oltra, J. E. Water: the ideal hydrogen-atom source in free-radical chemistry mediated by Ti^{III} and other single-electron-transfer metals? *Angew. Chem. Int. Ed.* **2006**, *45*, 5522-5526.
- (8) Nakano, Y.; Biegasiewicz, K. F.; Hyster, T. K. Biocatalytic hydrogen atom transfer: an invigorating approach to free-radical reactions. *Curr Opin Chem Biol* **2019**, *49*, 16-24.
- (9) (a) Kolmar, S. S.; Mayer, J. M. SmI₂(H₂O)_n reduction of electron rich enamines by proton-coupled electron transfer. *J. Am. Chem. Soc.* **2017**, *139*, 10687-10692. (b) Tarantino, K. T.; Miller, D. C.; Callon, T. A.; Knowles, R. R. Bond-weakening catalysis: conjugate aminations enabled by the soft homolysis of strong N-H bonds. *J. Am. Chem. Soc.* **2015**, *137*, 6440-6443. (c) Park, Y.; Kim, S.; Tian, L.; Zhong, H.; Scholes, G. D.; Chirik, P. J. Visible light enables catalytic formation of weak chemical bonds with molecular hydrogen. *Nat. Chem.* **2021**, *13*, 969-976.
- (10) (a) Ashida, Y.; Arashiba, K.; Nakajima, K.; Nishibayashi, Y. Molybdenum-catalysed ammonia production with samarium diiodide and alcohols or water. *Nature* **2019**, *568*, 536-540. (b) Zhang, Y.-Q.; Jakoby, V.; Stainer, K.; Schmer, A.; Klare, S.; Bauer, M.; Grimme, S.; Cuerva, J. M.; Gansäuer, A. Amide-substituted titanocenes in hydrogen-atom transfer catalysis. *Angew. Chem. Int. Ed.* **2016**, *55*, 1523-1526. (c) Paradas, M.; Campaña, A. G.; Jiménez, T.; Robles, R.; Oltra, J. E.; Buñuel, E.; Justicia, J.; Cárdenas, D. J.; Cuerva, J. M. Understanding the exceptional hydrogen-atom donor characteristics of water in Ti^{III}-mediated free-radical chemistry. *J. Am. Chem. Soc.* **2010**, *132*, 12748-12756.
- (11) (a) Fang, H.; Ling, Z.; Lang, K.; Brothers, P. J.; de Bruin, B.; Fu, X. Germanium(III) corrole complex: reactivity and mechanistic studies of visible-light promoted N-H bond activations. *Chem. Sci.* **2014**, *5*, 916-921. (b) Spiegel, D. A.; Wiberg, K. B.; Schacherer, L. N.; Medeiros, M. R.; Wood, J. L. Deoxygenation of alcohols employing water as the hydrogen atom source. *J. Am. Chem. Soc.* **2005**, *127*, 12513-12515. (c) Tantawy, W.; Zipse, H. Hydroxylic solvents as hydrogen atom donors in radical reactions. *Eur. J. Org. Chem.* **2007**, *2007*, 5817-5820. (d) Povie, G.; Marzorati, M.; Bigler, P.; Renaud, P. Role of equilibrium associations on the hydrogen atom transfer from the triethylborane-methanol complex. *J. Am. Chem. Soc.* **2013**, *135*, 1553-1558. (e) Wong, A.; Chakraborty, A.; Bawari, D.; Wu, G.; Dobrovetsky, R.; Ménard, G. Facile proton-coupled electron transfer enabled by coordination-induced E-H bond weakening to boron. *Chemical Communications* **2021**, *57*, 6903-6906.
- (12) (a) Liu, L.; Cao, L. L.; Shao, Y.; Ménard, G.; Stephan, D. W. A radical mechanism for frustrated Lewis pair reactivity. *Chem* **2017**, *3*, 259-267. (b) Dasgupta, A.; Richards, E.; Melen, R. L. Frustrated radical pairs: insights from EPR spectroscopy. *Angew. Chem. Int. Ed.* **2021**, *60*, 53-65.
- (13) Fang, H.; Jing, H.; Ge, H.; Brothers, P. J.; Fu, X.; Ye, S. The mechanism of E-H (E = N, O) bond activation by a germanium corrole complex: a combined experimental and computational study. *J. Am. Chem. Soc.* **2015**, *137*, 7122-7127.
- (14) de Marcillac, P.; Coron, N.; Dambier, G.; Leblanc, J.; Moalic, J.-P. Experimental detection of α-particles from the radioactive decay of natural bismuth. *Nature* **2003**, *422*, 876-878.
- (15) Planas, O.; Wang, F.; Leutzsch, M.; Cornella, J. Fluorination of arylboronic esters enabled by bismuth redox catalysis. *Science* **2020**, *367*, 313-317.
- (16) Ramler, J.; Krummenacher, I.; Lichtenberg, C. Bismuth compounds in radical catalysis: transition metal bismuthanes facilitate thermally induced cycloisomerizations. *Angew. Chem. Int. Ed.* **2019**, *58*, 12924-12929.
- (17) Pyykko, P. Relativistic effects in structural chemistry. *Chem. Rev.* **1988**, *88*, 563-594.
- (18) Power, P. P. Persistent and Stable Radicals of the Heavier Main Group Elements and Related Species. *Chem. Rev.* **2003**, *103*, 789-810.
- (19) (a) Casely, I. J.; Ziller, J. W.; Fang, M.; Furche, F.; Evans, W. J. Facile bismuth-oxygen bond cleavage, C-H activation, and formation of a monodentate carbon-bound oxyaryl dianion, (C₆H₂Bu₂-3,5-O-4)²⁻. *J. Am. Chem. Soc.* **2011**, *133*, 5244-5247. (b) Schwamm, R. J.; Harmer, J. R.; Lein, M.; Fitchett, C. M.; Granville, S.; Coles, M. P. Isolation and characterization of a bismuth(II) radical. *Angew. Chem. Int. Ed.* **2015**, *54*, 10630-10633. (c) Hanna, T. A.; Rieger, A. L.; Rieger, P. H.; Wang, X. Evidence for an unstable Bi(II) radical from Bi-O bond homolysis. Implications in the rate-determining step of the SOHIO process. *Inorg. Chem.* **2002**, *41*, 3590-3592. (d) Oberdorf, K.; Hanft, A.; Ramler, J.; Krummenacher, I.; Bickelhaupt, F. M.; Poater, J.; Lichtenberg, C. Bismuth amides mediate facile and highly selective Pn-Pn radical-coupling reactions (Pn=N, P, As). *Angew. Chem. Int. Ed.* **2021**, *60*, 6441-6445. (e) Hering-Junghans, C.; Schulz, A.; Thomas, M.; Villinger, A. Synthesis of mono-, di-, and triaminobismuthanes and observation of C-C coupling of aromatic systems with bismuth(III) chloride. *Dalton Trans.* **2016**, *45*, 6053-6059. (f) Ishida, S.; Hirakawa, F.; Furukawa, K.; Yoza, K.; Iwamoto, T. Frontispiece: persistent antimony- and bismuth-centered radicals in solution. *Angew. Chem. Int. Ed.* **2014**, *53*, 11172-11176. (g) Yamago, S.; Kayahara, E.; Kotani, M.; Ray, B.; Kwak, Y.; Goto, A.; Fukuda, T. Highly controlled living radical polymerization through dual activation of organobismuthines. *Angew. Chem. Int. Ed.* **2007**, *46*, 1304-1306.
- (20) Schwamm, R. J.; Lein, M.; Coles, M. P.; Fitchett, C. M. Catalytic oxidative coupling promoted by bismuth TEMPOxide complexes. *Chem. Commun.* **2018**, *54*, 916-919.
- (21) Wirlinga, U.; Roesky, H. W.; Noltemeyer, M.; Schmidt, H.-G. Synthesis and structure of a cyclic bismuth amide. *Inorg. Chem.* **1994**, *33*, 4607-4608.
- (22) Kou, X.; Wang, X.; Mendoza-Espinosa, D.; Zakharov, L. N.; Rheingold, A. L.; Watson, W. H.; Brien, K. A.; Jayarathna, L. K.; Hanna, T. A. Bismuth aryloxides. *Inorg. Chem.* **2009**, *48*, 11002-11016.
- (23) Janzen, E. G.; Wilcox, A. L.; Manoharan, V. Reactions of nitric oxide with phenolic antioxidants and phenoxyl radicals. *J. Org. Chem.* **1993**, *58*, 3597-3599.
- (24) (a) Neese, F. The ORCA program system. *WIREs Comput Mol Sci* **2012**, *2*, 73-78. (b) Neese, F.; Wennmohs, F.; Becker, U.; Riplinger, C. The ORCA quantum chemistry program package. *J. Chem. Phys.* **2020**, *152*, 224108-224118.
- (25) Pang, Y.; Leutzsch, M.; Nöthling, N.; Cornella, J. Catalytic activation of N₂O at a low-valent bismuth redox platform. *J. Am. Chem. Soc.* **2020**, *142*, 19473-19479.
- (26) Nekoueishahraki, B.; Sarish, S. P.; Roesky, H. W.; Stern, D.; Schulzke, C.; Stalke, D. Addition of dimethylaminobismuth to aldehydes, ketones, alkenes, and alkynes. *Angew. Chem. Int. Ed.* **2009**, *48*, 4517-4520.
- (27) Paiva, S.-L. Finding reverse. *Nat Rev Chem* **2021**, *5*, 751-751.
- (28) Pappas, I.; Chirik, P. J. Catalytic proton coupled electron transfer from metal hydrides to titanocene amides, hydrazides and imides: determination of thermodynamic parameters relevant to nitrogen fixation. *J. Am. Chem. Soc.* **2016**, *138*, 13379-13389.
- (29) (a) Schmidbaur, H.; Mitschke, K.-H. Darstellung und thermischer Zerfall von Vertretern des Typs R₃Sb(SR)₂. *Chem. Ber.* **1971**, *104*, 1842-

1846. (b) Bochmann, M.; Song, X.; Hursthouse, M. B.; Karaulov, A. Chalcogenolato complexes of bismuth and antimony. Syntheses, thermolysis reactions, and crystal structure of $\text{Sb}(\text{SC}_6\text{H}_2\text{Pr}^{i3-2,4,6})_3$. *J. Chem. Soc., Dalton Trans.* **1995**, 1649-1652.
- (30) Procacci, B.; Jiao, Y.; Evans, M. E.; Jones, W. D.; Perutz, R. N.; Whitwood, A. C. Activation of B–H, Si–H, and C–F bonds with $\text{Tp}^*\text{Rh}(\text{PMe}_3)$ complexes: kinetics, mechanism, and selectivity. *J. Am. Chem. Soc.* **2015**, *137*, 1258-1272.
- (31) (a) Vicha, J.; Novotný, J.; Komorovsky, S.; Straka, M.; Kaupp, M.; Marek, R. Relativistic heavy-neighbor-atom effects on NMR shifts: concepts and trends across the periodic table. *Chem. Rev.* **2020**, *120*, 7065-7103. (b) Olaru, M.; Duvinage, D.; Lork, E.; Mebs, S.; Beckmann, J. Heavy carbene analogues: donor-free bismuthenium and stibenium ions. *Angew. Chem. Int. Ed.* **2018**, *57*, 10080-10084. (c) Pang, Y.; Leutzsch, M.; Nöthling, N.; Katzenburg, F.; Cornella, J. Catalytic hydrodefluorination via oxidative addition, ligand metathesis, and reductive elimination at Bi(I)/Bi(III) centers. *J. Am. Chem. Soc.* **2021**, *143*, 12487-12493.
- (32) (a) Rodríguez-Lugo, R. E.; Trincado, M.; Vogt, M.; Tewes, F.; Santiso-Quinones, G.; Grützmacher, H. A homogeneous transition metal complex for clean hydrogen production from methanol–water mixtures. *Nat. Chem.* **2013**, *5*, 342-347. (b) Greb, L.; Ebner, F.; Ginzburg, Y.; Sigmund, L. M. Element-ligand cooperativity with p-block elements. *Eur. J. Inorg. Chem.* **2020**, *2020*, 3030-3047.
- (33) Semproni, S. P.; Milsmann, C.; Chirik, P. J. Four-coordinate cobalt pincer complexes: electronic structure studies and ligand modification by homolytic and heterolytic pathways. *J. Am. Chem. Soc.* **2014**, *136*, 9211-9224.
-